

Nonlinear formulation and free vibration of a large-sag extensible catenary riser

Ong-art Punjarat* and Somchai Chucheepsakul

*Department of Civil Engineering,
King Mongkut's University of Technology Thonburi, Bangkok, Thailand*

(Received November 27, 2019, Revised January 24, 2021, Accepted January 27, 2021)

Abstract. The nonlinear formulation using the principle of virtual work-energy for free vibration of a large-sag extensible catenary riser in two dimensions is presented in this paper. A support at one end is hinged and the other is a free-sliding roller in the horizontal direction. The catenary riser has a large-sag configuration in the static equilibrium state and is assumed to displace with large amplitude to the motion state. The total virtual work of the catenary riser system involves the virtual strain energy due to bending, the virtual strain energy due to axial deformation, the virtual work done by the effective weight, and the inertia forces. The nonlinear equations of motion for two-dimensional free vibration in the Cartesian coordinate system is developed based on the difference between the Euler's equations in the static state and the displaced state. The linear and nonlinear stiffness matrices of the catenary riser are obtained and the eigenvalue problem is solved using the Galerkin finite element procedure. The natural frequencies and mode shapes are obtained. The results are validated with regard to the reference research addressing the accuracy and efficiency of the proposed nonlinear formulation. The numerical results for free vibration and the effect of the nonlinear behavior for catenary riser are presented.

Keywords: axial deformation; catenary riser; free vibration; large amplitude; variational method

1. Introduction

A catenary riser is used for connecting the wellhead at the seafloor and a fixed or floating platform on the water surface. It is commonly used offshore in deep water for conveying fluids such as oil, gas, or injection fluid. During its lifetime of operation, the catenary riser is designed to sustain extreme external loads and severe environmental condition which induce internal stresses and motions (Zou 2012). The natural frequencies and mode shapes of the catenary riser are important dynamic properties and are the significant parameters used for the design stage. At present, most research on catenary risers is limited to large-sag catenary risers with a small amplitude of vibration. To the authors' knowledge, there is no example in the literature of a large sag with large-amplitude vibration. Therefore, the purpose of this research is to develop a nonlinear formulation using the principle of virtual work-energy for large-amplitude free vibration of a large-sag extensible catenary

*Corresponding author, Ph.D. Candidate, E-mail: ongart.punjarat@gmail.com

^a Professor, E-mail: somchai.chu@kmutt.ac.th

riser in two dimensions. A literature review of research related to catenary risers is presented in this paper.

A static analysis of a steel catenary riser subjected to its own self-weight was conducted by Moe and Arntsen (2001). Their model considered both inextensible and extensible risers. The numerical result was compared to the finite element method. A mathematical formulation for large-strain, extensible, flexible marine pipes transporting fluid was presented by Chucheepsakul *et al.* (2003). The virtual work principle and the vectorial method considering both Cartesian and natural coordinates for the large-strain formulations were developed. Kaewunruen *et al.* (2005) presented an investigation of the nonlinear natural frequencies and corresponding mode shapes for the marine pipe and riser. The virtual work-energy functional involves the bending strain energy, axial deformation strain energy, virtual work due to effective tension and external forces, and the kinetic energy due to riser and fluid motions. Their nonlinear equations of motion were derived using Hamilton's principle. Static and dynamic behavior of extensible marine risers due to the effect of the transporting fluid were investigated by Monprapussorn *et al.* (2007). The velocity of the internal flow of the transported fluid was considered as a constant, linear, or pulsatile flow. Their large-strain formulation was generated using the virtual work method and the vectorial method, and the numerical results were obtained using the finite element method.

Chatjigeorgiou (2008) proposed a finite difference solution for the simplified linear and nonlinear dynamic analysis of the catenary riser. The numerical results for static and dynamic responses were presented. Srinil *et al.* (2009a) and Srinil *et al.* (2009b) investigated a vortex-induced vibration of a catenary riser subjected to ocean current forces. Their riser was modeled using a pinned-pinned beam-cable model with bending and extensibility stiffness. Various behaviors of the response amplitude diagram, such as multimode lock-in, switching, sharing, and interaction features, were described. Athisakul *et al.* (2011) adopted a variational approach to solve the extensible three-dimensional, large-displacement marine riser in static and dynamic states based on the work-energy principle. Their model formulation has the flexibility of independent variables such as water depth, offset, or the arc-length coordinate in Cartesian coordinates. The virtual work-energy involves the bending and axial deformation strain energy, torsion, and the virtual work done by the external and internal fluid. The numerical results were obtained using the finite element method.

The static configurations of a steel catenary riser were investigated by Athisakul *et al.* (2014) using the variational formulation and the finite element method. Their research reported the unstable and stable configurations of the riser exhibited when the applied top tension was higher or lower than the critical top tension. Klaycham *et al.* (2014) proposed the nonlinear free vibration analysis of a steel catenary riser transporting fluid based on Hamilton's principle. The work-energy functional involves the bending and axial deformation strain energy and the work done by inertia forces of the riser and transporting fluid motion. The large-amplitude free vibration with various horizontal offsets and top tensions were studied and reported. Klaycham *et al.* (2016) investigated the nonlinear free vibration of a two-dimensional marine riser with large displacement. The variational formulation was developed using Hamilton's principle and the finite element method was employed to obtain the numerical solution. Klaycham (2016) presented a nonlinear vibration analysis with large-amplitude motions for the extensible marine riser. His variational and finite element model were formulated with variables of x and y and arc length coordinates. The dynamic characteristics of the marine riser were presented. The study also evaluated the dynamic responses induced by various loads, such as hydrodynamic wave, current, and unsteady flow of internal transported fluid. Klaycham *et al.* (2020) presented the free vibration analysis of a large sag catenary

shape with application to catenary jumper in hybrid riser system using the variational formulation and the finite element method.

Alfosail *et al.* (2017) used the Galerkin approach to extract mode shapes and the natural frequencies of the inclined marine risers. The riser was modeled by the Euler-Bernoulli beam and the nonlinear stretch at midplane was considered. The significance of including the bending moment in the static and dynamic analysis of the risers was addressed. Kim and O'Reilly (2019) studied the instability of the static and vibration states of a flexible riser conveying fluid. Their three-dimensional riser model can be either extensible or inextensible; the riser has pinned-pinned ends support. Numerical solution by the finite difference method was used to obtain the static configuration of the riser and a parametric study on the effects of the internal flow and current on the stability and dynamic behavior carried out.

2. Variational model formulation

The three states of the large-sag extensible catenary riser configuration in two dimensions, that is, undeformed, static, and dynamic states, are illustrated in Fig. 1. The catenary riser is modeled between the hinged support at one end and a free-sliding roller support in the horizontal direction at the other end. The lowest point of the large sag configuration may be not at the same level at the lower end. Thus, the touchdown zone may not exist and it is not considered in the model formulation. The influence of touchdown zone on the natural frequencies of riser is a localized problem due to the boundary layer effect (Pesce *et al.* 1998, Klaycham *et al.* 2016).

The principle of work-energy in a two-dimensional Cartesian coordinate system is employed to develop the variational formulation of the mechanical behavior of the catenary riser induced by the applied force and environmental load. The virtual work for the static analysis involves the bending strain energy, the virtual work done by the top horizontal tension force, the effective weight, and the current drag force. The bending behavior of the catenary riser follows Euler-Bernoulli beam theory, in which deformation due to shear effect is neglected (Punjarat and Chucheepsakul 2019a). The virtual work for dynamic analysis involves the bending strain energy, the axial deformation strain energy, the virtual work done of the effective weight and inertia force. The arc-length coordinate of the catenary riser is used as an independent variable in the nonlinear formulation.

As shown in Fig. 1, the geometrical configuration of the catenary riser in three states provided the following relations:

$$\sin\theta = \frac{dy_0}{ds_0} = \frac{y_0'}{s_0'} \quad (1a)$$

$$\cos\theta = \frac{dx_0}{ds_0} = \frac{x_0'}{s_0'} \quad (1b)$$

$$s_0'^2 = x_0'^2 + y_0'^2 \quad (1c)$$

The prime symbol (') represents the derivative with respect to the catenary riser unstrained arc length \bar{s} , the subscript (s_0) defines the unstrained arc length in the equilibrium state, the angle (θ) is measured between the arc length of the catenary riser and the horizontal. The curvature (κ) of the catenary riser element can be obtained by differentiating Eq. (1(a)) with respect to the catenary riser arc-length parameter s_0 and gives

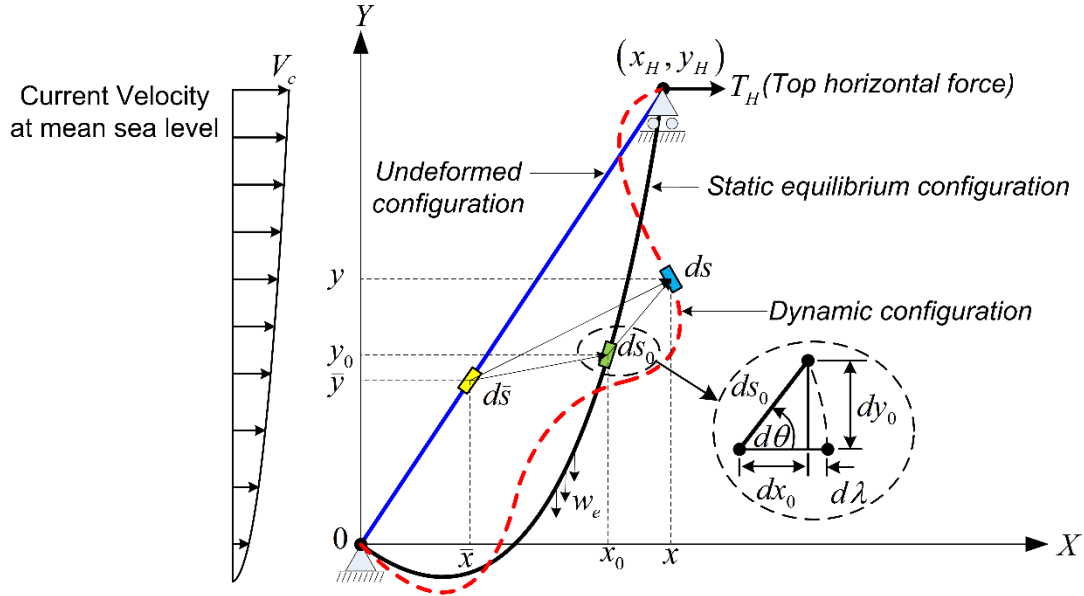


Fig. 1 Configuration of the catenary riser in three states

$$\kappa = \frac{d\theta}{ds_0} = \frac{y_0''}{(1-y_0'^2)^{\frac{1}{2}}} \quad (2)$$

The total axial strain (ε_0) of the extensible catenary riser in the equilibrium state can be expressed by

$$\varepsilon_0 = \frac{ds_0 - d\bar{s}}{d\bar{s}} \quad (3)$$

The catenary riser arc length in the static equilibrium state ds_0 can be expressed in terms of the Cartesian coordinate components (x_0, y_0) by

$$ds_0 = (1 + \varepsilon_0)d\bar{s} = \sqrt{x_0'^2 + y_0'^2}d\bar{s} \quad (4)$$

where $d\bar{s}$ is the infinitesimal arc length in the undeformed state. With Eqs. (1(c)) and (4), the following expression can be obtained

$$x_0' = \sqrt{(1 + \varepsilon_0)^2 - y_0'^2} \quad (5)$$

The total virtual work of the catenary riser in the static equilibrium state is composed of the bending strain energy, the external virtual work done due to the top horizontal tension force (T_H), the effective weight (w_e), and the current drag force, developed by Punjarat and Chucheeepsakul (2019a, b) as follows

$$\delta\pi = \int_0^{st} \left\{ \begin{array}{l} \frac{Ely_0''}{1-y_0'^2} \delta y_0'' + \frac{Ely_0' y_0''^2}{(1-y_0'^2)^2} \delta y_0' + T_H \frac{y_0'}{\sqrt{(1+\varepsilon_0)^2 - y_0'^2}} \delta y_0' \\ + w_e \delta y_0 + (f_{Hny} - f_{Hty}) \delta y_0 \end{array} \right\} d\bar{s} \quad (6)$$

where w_e is the effective weight; $w_e = (\rho_p A_p - \rho_e A_e + \rho_i A_i)g$, ρ_p, ρ_e and ρ_i are the densities of the riser pipe, external fluid, and internal fluid, respectively. A_p, A_e , and A_i are the cross-sectional areas of the riser pipe, outside diameter, and inside diameter, respectively, and g is the gravitational acceleration; f_{Hny} and f_{Hty} are the current drag force in the normal and tangential directions.

In dynamic analysis, the variational formulation based on the work-energy principle is developed which involves the bending strain energy, an axial deformation, and virtual work done due to effective weight and inertia force. The work-energy functional is developed in terms of the deformed arc-length coordinate of the catenary riser; the strain energy due to shear is neglected. The dynamic displacement from the static equilibrium state in horizontal and vertical directions in u and v of the Cartesian coordinate system, respectively, is illustrated in Fig. 2.

The arc length of the catenary riser at the stretched state, ds , can be expressed by

$$ds = \sqrt{(x_0' + u')^2 + (y_0' + v')^2} d\bar{s} \quad (7)$$

The strain in the displaced state, ε , followed the total Lagrangian description and can be expressed by

$$\varepsilon = \frac{ds - d\bar{s}}{d\bar{s}} = \sqrt{(x_0' + u')^2 + (y_0' + v')^2} - 1 \quad (8)$$

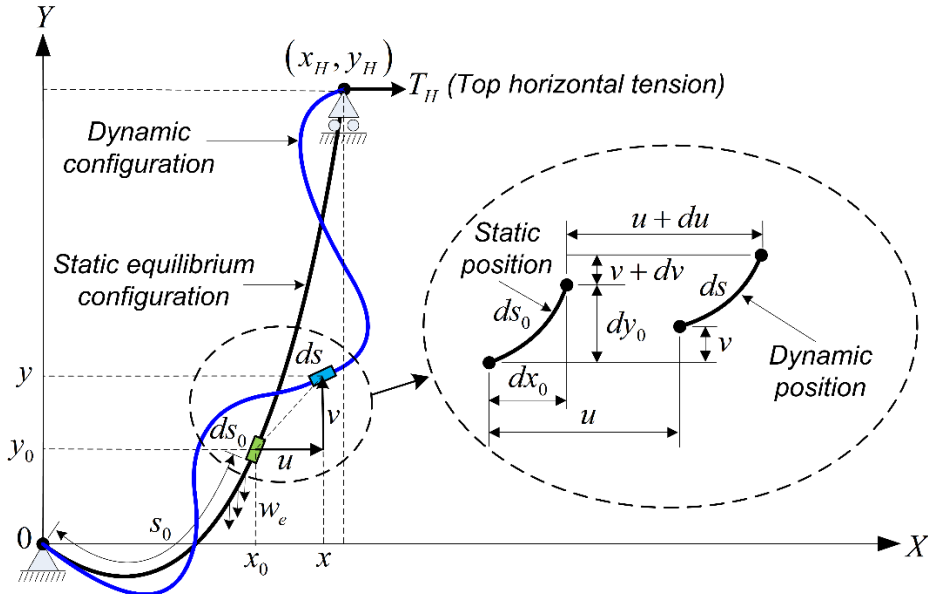


Fig. 2 Schematic of static and dynamic configurations of the catenary riser

Its derivative is

$$\delta\varepsilon = \frac{(x'_0+u')\delta u'+(y'_0+v')\delta v'}{\sqrt{(x'_0+u')^2+(y'_0+v')^2}} \quad (9)$$

2.1 Virtual strain energy due to axial deformation

The variation of the strain energy due to axial deformation can be expressed by

$$\delta U_a = \int_0^{s_t} EA\varepsilon(\delta\varepsilon)d\bar{s} \quad (10)$$

where E is the elastic modulus and A is the cross section of the catenary riser.

Substitution of Eqs. (8) and (9) into Eq. (10) gives

$$\delta U_a = \int_0^{s_t} EA(\sqrt{(x'_0+u')^2+(y'_0+v')^2}-1)\frac{(x'_0+u')\delta u'+(y'_0+v')\delta v'}{\sqrt{(x'_0+u')^2+(y'_0+v')^2}}d\bar{s} \quad (11)$$

The dynamic updated Green's strain γ_d , as given by Chucheepsakul *et al.* (2003), is

$$\gamma_d = \frac{x'_0u'+y'_0v'}{x_0'^2+y_0'^2} + \frac{1}{2}\frac{(u'^2+v'^2)}{(x_0'^2+y_0'^2)} = \frac{1}{(1+\varepsilon_0)^2}\left(x'_0u'+y'_0v'+\frac{1}{2}u'^2+\frac{1}{2}v'^2\right) \quad (12)$$

By approximation using the binomial series, and neglecting the higher-order terms for linearization purposes, one obtains

$$\frac{1}{\sqrt{1+2\gamma_d}} \approx 1 - \frac{1}{2}(2\gamma_d) + \frac{1}{2!}\left(-\frac{1}{2}\right)\left(-\frac{3}{2}\right)(2\gamma_d)^2 + \dots \approx 1 - \gamma_d \quad (13)$$

The arc length of the catenary riser in the stretched state can be simplified using Eq. (13), to give

$$\sqrt{(x'_0+u')^2+(y'_0+v')^2} = \sqrt{x_0'^2+y_0'^2+2(x'_0u'+y'_0v')+u'^2+v'^2} = \sqrt{1+2\gamma_d}(1+\varepsilon_0) \quad (14)$$

Substituting Eqs. (13) and (14) into Eq. (11), one obtains

$$\delta U_a = \int_0^{s_t} \frac{EA}{1+\varepsilon_0}(\varepsilon_0+\gamma_d)[(x'_0+u')\delta u'+(y'_0+v')\delta v']d\bar{s} \quad (15)$$

Rearranging Eq. (15) by using Eq. (12) and substituting the axial tension in the equilibrium state, $T = EA\varepsilon_0$, the virtual strain energy due to axial deformation is

$$\begin{aligned} \delta U_a = & \int_0^{s_t} \left[\frac{T}{1+\varepsilon_0} + \frac{EA}{(1+\varepsilon_0)^3} \left(x'_0u'+y'_0v'+\frac{1}{2}u'^2+\frac{1}{2}v'^2 \right) \right] (x'_0+u')\delta u'd\bar{s} \\ & + \int_0^{s_t} \left[\frac{T}{1+\varepsilon_0} + \frac{EA}{(1+\varepsilon_0)^3} \left(x'_0u'+y'_0v'+\frac{1}{2}u'^2+\frac{1}{2}v'^2 \right) \right] (y'_0+v')\delta v'd\bar{s} \end{aligned} \quad (16)$$

2.2 Strain energy due to bending

The bending strain energy presented in the total Lagrangian descriptor is defined by

$$\delta U_b = \int_0^{s_t} [M\delta(\theta' - \bar{\theta}')] d\bar{s} \quad (17)$$

while the bending moment can be expressed in terms of the curvature and dynamic strain, as follows:

$$M = EI[\kappa(1 + \varepsilon) - \bar{\kappa}] \quad (18)$$

The bending stiffness, EI , of the catenary riser is considered constant and the rotational angle in terms of the total strain is defined by

$$\theta' = \kappa(1 + \varepsilon) \quad (19)$$

with the assumption that the catenary riser is straight in the undeformed state, then $\bar{\theta}' = \bar{\kappa} = 0$. Thus, Eq. (17) is reduced to

$$\delta U_b = \int_0^{s_t} M\delta\theta' d\bar{s} \quad (20)$$

The curvature of the catenary riser in the displaced state can be expressed in terms of the Cartesian coordinate components (x, y) as the following equation

$$\theta' = \frac{x'y'' - x''y'}{x'^2 + y'^2} \quad (21)$$

Observing that $\sin\theta = dy/ds$ and $\cos\theta = dx/ds$, the derivative of the curvature in Eq. (21) can be expressed as

$$\delta\theta' = -\left(\frac{y'}{s'^2}\right)\delta u'' + \left(\frac{x'}{s'^2}\right)\delta v'' - \left(\kappa_0 \frac{x'}{s'} - \frac{x'x'' + y'y''}{s'^3} \left(\frac{y'}{s'}\right)\right)\delta u' - \left(\kappa_0 \frac{y'}{s'} + \frac{x'x'' + y'y''}{s'^3} \left(\frac{x'}{s'}\right)\right)\delta v' \quad (22)$$

Substituting Eqs. (21) and (22) into Eq. (17) yields the variational functional of the bending strain energy, as follows:

$$\begin{aligned} \delta U_b = & \int_0^{s_t} EI(1 + \varepsilon) \left\{ \begin{array}{l} (x'_0 + u')(y''_0 + v'') \\ -(x''_0 + u'')(y'_0 + v') \end{array} \right\} \left\{ \begin{array}{l} -(y'_0 + v')\delta u'' + (x'_0 + u')\delta v'' \\ -\kappa_0(x'_0 + u')\delta u' - \kappa_0(y'_0 + v')\delta v' \end{array} \right\} d\bar{s} \\ & + \int_0^{s_t} EI(1 + \varepsilon) \left\{ \begin{array}{l} (x'_0 + u')(x''_0 + u'') \\ +(y'_0 + v')(y''_0 + v'') \end{array} \right\} \kappa_0 \left\{ (y'_0 + v')\delta u' - (x'_0 + u')\delta v' \right\} d\bar{s} \quad (23) \end{aligned}$$

The expression of s' in Eq. (22) vanishes once the work-energy functional in this study is formulated in terms of the catenary riser arc length coordinate.

2.3 Virtual work due to effective weight and inertia forces

The virtual work done due to effective weight and inertia forces can be expressed by

$$\delta W_a = - \int_0^{s_t} w_e \left\{ \frac{\sqrt{x_0'^2 + y_0'^2}}{g(1+\varepsilon_0)} \ddot{u} \delta u + \left(\frac{\sqrt{x_0'^2 + y_0'^2}}{1+\varepsilon_0} + \frac{\sqrt{x_0'^2 + y_0'^2}}{g(1+\varepsilon_0)} \ddot{v} \right) \delta v \right\} d\bar{s} \quad (24)$$

where w_e is the effective weight; $w_e = (\rho_p A_p + \rho_i A_i + \rho_e A_e C_a)g$ and C_a is the added mass coefficient; \ddot{u} and \ddot{v} are the acceleration in x and y directions, respectively.

3. Equations of motion

The total virtual work-energy of the catenary riser system can be defined by

$$\delta \Pi = \delta U_a + \delta U_b - \delta W_a = 0 \quad (25)$$

Substitution of Eqs. (16), (23), and (24) into Eq. (25) yields the expression of total virtual work, as follows

$$\begin{aligned} \Pi = \int_0^{s_t} & \left\{ \begin{aligned} & \left[\frac{T}{1+\varepsilon_0} + \frac{EA}{(1+\varepsilon_0)^3} (x_0' u' + y_0' v' + \frac{1}{2} u'^2 + \frac{1}{2} v'^2) \right] (x_0' + u') \delta u' \\ & -EI(1+\varepsilon) [(x_0' + u')(y_0'' + v'') - (x_0'' + u'')(y_0' + v')] (y_0' + v') \delta u'' \\ & -EI(1+\varepsilon) \kappa_0 [(x_0' + u')(y_0'' + v'') - (x_0'' + u'')(y_0' + v')] (x_0' + u') \delta u' \\ & +EI(1+\varepsilon) \kappa_0 [(x_0' + u')(x_0'' + u'') + (y_0' + v')(y_0'' + v'')] (y_0' + v') \delta u' \\ & + \left(w_e \frac{\sqrt{x_0'^2 + y_0'^2}}{g(1+\varepsilon_0)} \ddot{u} \right) \delta u \end{aligned} \right\} d\bar{s} \\ + \int_0^{s_t} & \left\{ \begin{aligned} & \left[\frac{T}{1+\varepsilon_0} + \frac{EA}{(1+\varepsilon_0)^3} (x_0' u' + y_0' v' + \frac{1}{2} u'^2 + \frac{1}{2} v'^2) \right] (y_0' + v') \delta v' \\ & +EI(1+\varepsilon) [(x_0' + u')(y_0'' + v'') - (x_0'' + u'')(y_0' + v')] (x_0' + u') \delta v'' \\ & -EI(1+\varepsilon) \kappa_0 [(x_0' + u')(y_0'' + v'') - (x_0'' + u'')(y_0' + v')] (y_0' + v') \delta v' \\ & -EI(1+\varepsilon) \kappa_0 [(x_0' + u')(x_0'' + u'') + (y_0' + v')(y_0'' + v'')] (x_0' + u') \delta v' \\ & + \left(w_e \frac{\sqrt{x_0'^2 + y_0'^2}}{1+\varepsilon_0} + w_e \frac{\sqrt{x_0'^2 + y_0'^2}}{g(1+\varepsilon_0)} \ddot{v} \right) \delta v \end{aligned} \right\} d\bar{s} \quad (26) \end{aligned}$$

Applying integration by part twice to obtain the equation of motion for the extensible catenary riser and considering the catenary riser in static equilibrium state, $\delta \pi = 0$ and $u = v = u' = v' = u'' = v'' = \varepsilon = 0$. The Euler equation in Eq. (26) in u and v directions is reduced to

$$-\frac{T}{1+\varepsilon_0} (x_0')' - EI(x_0' y_0' y_0'' - x_0'' y_0'^2)'' + EI \kappa_0 (x_0'^2 y_0'' - 2x_0' x_0'' y_0' - y_0'^2 y_0'')' = 0 \quad (27)$$

and

$$-\frac{T}{1+\varepsilon_0}(y'_0)' + EI(x_0'^2 y_0'' - x_0' x_0'' y_0')'' + EI\kappa_0(2x_0' y_0' y_0'' - x_0'' y_0'^2 + x_0'^2 x_0'')' = 0 \quad (28)$$

For the catenary riser in motion, $u \neq 0, v \neq 0, u' \neq 0, v' \neq 0, u'' \neq 0, v'' \neq 0$. The Euler equation in u and v directions becomes

$$\begin{aligned} & -\frac{T}{1+\varepsilon_0}(x'_0 + u')' - \frac{EA}{(1+\varepsilon_0)^3} \left(x_0'^2 u' + x_0' y_0' v' + \frac{1}{2} x_0' u'^2 + \frac{1}{2} x_0' v'^2 \right)' \\ & -EI \left(x_0' y_0' y_0'' + y_0' y_0'' u' + x_0' y_0' v'' + y_0' u' v'' - x_0'' y_0'^2 - y_0'^2 u'' - 2x_0'' y_0' v' - 2y_0' u'' v' \right)'' \\ & + x_0' y_0'' v' + y_0'' u' v' + x_0' v' v'' + u' v' v'' - x_0'' v'^2 - u'' v'^2 \\ & +EI\kappa_0 \left(x_0'^2 y_0'' + x_0' y_0'' u' + x_0'^2 v'' + 2x_0' u' v'' - x_0' x_0'' y_0' - x_0' y_0' u'' - x_0' x_0'' v' - x_0' u'' v' \right)' \\ & + x_0' y_0'' u' + y_0'' u'^2 + u'^2 v'' - x_0'' y_0' u' - y_0' u'' u' - x_0'' u' v' - u'' u' v' \\ & -EI\kappa_0 \left(x_0' x_0'' y_0' + x_0'' y_0' u' + x_0' y_0' u'' + y_0' u' u'' + y_0'^2 y_0'' + 2y_0' y_0'' v' + y_0'^2 v'' \right)' \\ & + 2y_0' v' v'' + y_0'' v'^2 + x_0' x_0'' v' + x_0'' u' v' + x_0' u'' v' + v'^2 v'' + u' u'' v' \end{aligned} + w_e \frac{\sqrt{x_0'^2 + y_0'^2}}{g(1+\varepsilon_0)} \ddot{u} = 0 \quad (29)$$

and

$$\begin{aligned} & -\frac{T}{1+\varepsilon_0}(y'_0 + v')' - \frac{EA}{(1+\varepsilon_0)^3} \left(x_0' y_0' u' + y_0'^2 v' + \frac{1}{2} y_0' u'^2 + \frac{1}{2} y_0' v'^2 \right)' \\ & +EI \left(x_0'^2 y_0'' + 2x_0' y_0'' u' + x_0'^2 v'' + 2x_0' u' v'' - x_0' x_0'' y_0' - x_0' y_0' u'' - x_0' x_0'' v' - x_0' u'' v' \right)'' \\ & + y_0'' u'^2 + u'^2 v'' - x_0'' y_0' u' - y_0' u'' u' - x_0'' u' v' - u'' u' v' \\ & +EI\kappa_0 \left(x_0' y_0' y_0'' + y_0' y_0'' u' + x_0' y_0' v'' + y_0' u' v'' - x_0'' y_0'^2 - y_0'^2 u'' - 2x_0'' y_0' v' - 2y_0' u'' v' \right)' \\ & + x_0' y_0'' v' + y_0'' u' v' + x_0' v' v'' + u' v' v'' - x_0'' v'^2 - u'' v'^2 \\ & +EI\kappa_0 \left(x_0'^2 x_0'' + 2x_0' x_0'' u' + x_0'^2 u'' + 2x_0' u' u'' + x_0' y_0' y_0'' + x_0' y_0'' v' + x_0' y_0' v'' + x_0' v' v'' \right)' \\ & + x_0'' u'^2 + u'^2 u'' + y_0' y_0'' u' + y_0'' u' v' + y_0' u' v'' + u' v' v'' \end{aligned} + w_e \frac{\sqrt{x_0'^2 + y_0'^2}}{1+\varepsilon_0} + w_e \frac{\sqrt{x_0'^2 + y_0'^2}}{g(1+\varepsilon_0)} \ddot{v} = 0 \quad (30)$$

Subtracting Eq. (27) from Eq. (29) and subtracting Eq. (28) from Eq. (30), one obtains the equations of motion for a large-sag extensible catenary riser in u and v directions, respectively. This can be written as

$$m_u \ddot{u} + f_1(u'', v'') + f_2(u''', v''') + f_3(u^{iv}, v^{iv}) = 0 \quad (31)$$

and

$$m_v \ddot{v} + g_1(u'', v'') + g_2(u''', v''') + g_3(u^{iv}, v^{iv}) = 0 \quad (32)$$

Neglecting the higher-order terms in Eqs. (29) and (30), the linear and nonlinear stiffness matrix coefficients, f_1, f_2, \dots, g_3 , in Eqs. (31) and (32), can be expressed as follows

$$f_1(u'', v'') = \frac{Tu''}{1+\varepsilon_0} + \frac{EA}{(1+\varepsilon_0)^3} \begin{pmatrix} x_0'^2 u'' + x_0' y_0' v'' \\ +(3x_0' u' + y_0' v') u'' + (x_0' v' + y_0' u') v'' \\ + \left(\frac{3}{2} u'^2 + \frac{1}{2} v'^2\right) u'' + u' v' v'' \end{pmatrix} \quad (33)$$

$$f_2(u''', v''') = -EI\kappa_0 \begin{pmatrix} -2x_0' y_0' u''' + (x_0'^2 - y_0'^2) v''' + (-2y_0' u' - 2x_0' v') u''' \\ +(2x_0' u' - 2y_0' v') v''' - 2u' v' u''' + (u'^2 - v'^2) v''' \end{pmatrix} \quad (34)$$

$$f_3(u^{iv}, v^{iv}) = EI \begin{pmatrix} -y_0'^2 u^{iv} + x_0' y_0' v^{iv} - 2y_0' v' u^{iv} + (y_0' u' + x_0' v') v^{iv} \\ -v'^2 u^{iv} + u' v' v^{iv} \end{pmatrix} \quad (35)$$

$$g_1(u'', v'') = \frac{Tv''}{1+\varepsilon_0} + \frac{EA}{(1+\varepsilon_0)^3} \begin{pmatrix} x_0' y_0' u'' + y_0'^2 v'' \\ +(x_0' v' + y_0' u') u'' + (3y_0' v' + x_0' u') v'' \\ + u' v' u'' + \left(\frac{1}{2} u'^2 + \frac{3}{2} v'^2\right) v'' \end{pmatrix} \quad (36)$$

$$g_2(u''', v''') = -EI\kappa_0 \begin{pmatrix} (x_0'^2 - y_0'^2) u''' + 2x_0' y_0' v''' + (2x_0' u' - 2y_0' v') u''' \\ +(2x_0' v' + 2y_0' u') v''' + (u'^2 - v'^2) u''' + 2u' v' v''' \end{pmatrix} \quad (37)$$

$$g_3(u^{iv}, v^{iv}) = -EI \begin{pmatrix} -x_0' y_0' u^{iv} + x_0'^2 v^{iv} - (x_0' v' + y_0' u') u^{iv} + 2x_0' u' v^{iv} \\ -u' v' u^{iv} + u'^2 v^{iv} \end{pmatrix} \quad (38)$$

3.1 Linear free vibration

The linear free vibration of the large-sag extensible catenary riser can be expressed by

$$\begin{bmatrix} m_u & 0 \\ 0 & m_v \end{bmatrix} \begin{Bmatrix} \ddot{u} \\ \ddot{v} \end{Bmatrix} + [\mathbf{k}_L] \begin{Bmatrix} u'' \\ v'' \end{Bmatrix} + [\mathbf{k}_L] \begin{Bmatrix} u''' \\ v''' \end{Bmatrix} + [\mathbf{k}_L] \begin{Bmatrix} u^{iv} \\ v^{iv} \end{Bmatrix} = \{\mathbf{0}\} \quad (39)$$

where the mass of the catenary riser in u and v directions is defined by

$$m_u = m_v = w_e \frac{\sqrt{x_0'^2 + y_0'^2}}{g(1+\varepsilon_0)} \quad (40)$$

The linear axial stiffness matrix of the second-order derivative is

$$[\mathbf{k}_L^a] = \begin{bmatrix} \frac{T}{1+\varepsilon_0} + \frac{EAx_0'^2}{(1+\varepsilon_0)^3} & \frac{EAx_0'y_0'}{(1+\varepsilon_0)^3} \\ \frac{EAx_0'y_0'}{(1+\varepsilon_0)^3} & \frac{T}{1+\varepsilon_0} + \frac{EAy_0'^2}{(1+\varepsilon_0)^3} \end{bmatrix} \quad (41)$$

The linear bending stiffness matrix of the fourth-order derivative is

$$[\mathbf{k}_L^{b1}] = EI \begin{bmatrix} -y_0'^2 & x_0'y_0' \\ x_0'y_0' & -x_0'^2 \end{bmatrix} \quad (42)$$

The linear bending stiffness matrix of the third-order derivative is

$$[\mathbf{k}_L^{b2}] = EI\kappa_0 \begin{bmatrix} 2x_0'y_0' & y_0'^2 - x_0'^2 \\ y_0'^2 - x_0'^2 & -2x_0'y_0' \end{bmatrix} \quad (43)$$

3.2 Nonlinear free vibration

The nonlinear free vibration of the large-sag extensible catenary riser can be expressed by

$$\begin{bmatrix} m_u & 0 \\ 0 & m_v \end{bmatrix} \begin{Bmatrix} \ddot{u} \\ \ddot{v} \end{Bmatrix} + ([\mathbf{k}_L] + [\mathbf{k}_{NL}]) \begin{Bmatrix} u'' \\ v'' \end{Bmatrix} + ([\mathbf{k}_L] + [\mathbf{k}_{NL}]) \begin{Bmatrix} u''' \\ v''' \end{Bmatrix} + ([\mathbf{k}_L] + [\mathbf{k}_{NL}]) \begin{Bmatrix} u^{iv} \\ v^{iv} \end{Bmatrix} = \{\mathbf{0}\} \quad (44)$$

The first-order nonlinear axial stiffness matrix is

$$[\mathbf{k}_{NL}^{a1}] = \frac{EA}{(1+\varepsilon_0)^3} \begin{bmatrix} 3x_0'u' + y_0'v' & x_0'v' + y_0'u' \\ x_0'v' + y_0'u' & 3y_0'v' + x_0'u' \end{bmatrix} \quad (45)$$

The second-order nonlinear axial stiffness matrix is

$$[\mathbf{k}_{NL}^{a2}] = \frac{EA}{(1+\varepsilon_0)^3} \begin{bmatrix} \frac{3}{2}u'^2 + \frac{1}{2}v'^2 & u'v' \\ u'v' & \frac{3}{2}v'^2 + \frac{1}{2}u'^2 \end{bmatrix} \quad (46)$$

The first-order nonlinear bending stiffness matrix of the fourth-order derivative is

$$[\mathbf{k}_{NL}^{b1}] = EI \begin{bmatrix} -2y_0'v' & y_0'u' + x_0'v' \\ y_0'u' + x_0'v' & -2x_0'u' \end{bmatrix} \quad (47)$$

The second-order nonlinear bending stiffness matrix of the fourth-order derivative is

$$[\mathbf{k}_{NL}^{b2}] = EI \begin{bmatrix} -v'^2 & u'v' \\ u'v' & -u'^2 \end{bmatrix} \quad (48)$$

The first-order nonlinear bending stiffness matrix of the third-order derivative is

$$[\mathbf{k}_{NL}^{b3}] = 2EI\kappa_0 \begin{bmatrix} y_0'u' + x_0'v' & -x_0'u' + y_0'v' \\ -x_0'u' + y_0'v' & -y_0'u' - x_0'v' \end{bmatrix} \quad (49)$$

The second-order nonlinear bending stiffness matrix of the third-order derivative is

$$[\mathbf{k}_{NL}^{b4}] = EI\kappa_0 \begin{bmatrix} 2u'v' & -u'^2 + v'^2 \\ -u'^2 + v'^2 & -2u'v' \end{bmatrix} \quad (50)$$

4. Finite element method

The static equilibrium configuration for the large-sag extensible catenary riser was obtained in previous work by the authors using the finite element method and the Newton-Raphson iterative procedure (Punjarat and Chucheepsakul, 2019a, b). The equation of motion is solved using the Galerkin finite element method (Cook *et al.* 2002). The displacement components vector in two-dimensional Cartesian coordinate is written as

$$\{\mathbf{u}\} = \{u \ v\}^T \approx [\mathbf{N}]\{\mathbf{d}\} \quad (51)$$

where $[\mathbf{N}]$ is the cubic polynomial shape function matrix arranged in the form

$$[\mathbf{N}] = \begin{bmatrix} N_1 & N_2 & 0 & 0 & N_3 & N_4 & 0 & 0 \\ 0 & 0 & N_1 & N_2 & 0 & 0 & N_3 & N_4 \end{bmatrix} \quad (52)$$

and $\{\mathbf{d}\}$ is the nodal displacement coordinate, which is written as

$$\{\mathbf{d}\} = \{u_1 \ u'_1 \ v_1 \ v'_1 \ u_2 \ u'_2 \ v_2 \ v'_2\}^T \quad (53)$$

4.1 Linear free vibration solution

Eq. (39) can be written in the form of a matrix following the Galerkin finite element method, as follows

$$\begin{aligned} & \sum_{j=1}^{N_{elem}} \left(\int_0^l [\mathbf{N}]^T \begin{bmatrix} m_u & 0 \\ 0 & m_v \end{bmatrix} [\mathbf{N}] ds \{\ddot{\mathbf{d}}\} + \int_0^l [\mathbf{N}']^T \begin{bmatrix} k_{uu} & k_{uv} \\ k_{vu} & k_{vv} \end{bmatrix} [\mathbf{N}'] ds \{\mathbf{d}\} \right. \\ & \left. + \int_0^l [\mathbf{N}']^T \begin{bmatrix} k_{uu} & k_{uv} \\ k_{vu} & k_{vv} \end{bmatrix} [\mathbf{N}'] ds \{\mathbf{d}\} + \int_0^l [\mathbf{N}'']^T \begin{bmatrix} k_{uu} & k_{uv} \\ k_{vu} & k_{vv} \end{bmatrix} [\mathbf{N}''] ds \{\mathbf{d}\} \right) = \{\mathbf{0}\} \end{aligned} \quad (54)$$

where j is the element number and $[\mathbf{N}']$ and $[\mathbf{N}'']$ are the first and second derivatives, respectively, of the cubic polynomial shape functions.

The finite element equation of the global system for linear free vibration can be expressed by

$$[\mathbf{M}]\{\ddot{\mathbf{D}}\} + [\mathbf{K}_L]\{\mathbf{D}\} = \{\mathbf{0}\} \quad (55)$$

where $\{\ddot{\mathbf{D}}\}$ and $\{\mathbf{D}\}$ are the acceleration and displacement vectors, respectively, and can be obtained by assembling the element acceleration and displacements. Therefore

$$\{\mathbf{D}\} = \sum_{j=1}^{nelem} \{\mathbf{d}\} \quad (56a)$$

and

$$\{\ddot{\mathbf{D}}\} = \sum_{j=1}^{nelem} \{\ddot{\mathbf{d}}\} \quad (56b)$$

The global mass matrices $[\mathbf{M}]$ is defined by

$$[\mathbf{M}] = \sum_{j=1}^{Nelem} [\mathbf{m}] \quad (57)$$

where $[\mathbf{m}]$ is the element mass matrix, which is given by

$$[\mathbf{m}] = \int_0^l (m_p + m_i + C_a^*) [\mathbf{N}]^T \begin{bmatrix} 1 & 0 \\ 0 & 1 \end{bmatrix} [\mathbf{N}] ds \quad (58)$$

Here m_p, m_i , and C_a^* are the mass of the catenary riser, internal fluid, and the external fluid, including the added mass coefficient, respectively. The linear global stiffness matrix $[\mathbf{K}_L]$ is

$$[\mathbf{K}_L] = \sum_{j=1}^{Nelem} [\mathbf{k}_L] \quad (59)$$

where $[\mathbf{k}_L]$ is the element linear stiffness matrix, consisting of the linear axial stiffness matrix and linear bending stiffness matrices.

$$[\mathbf{k}_L] = [\mathbf{k}_L^a] + [\mathbf{k}_L^{b1}] + [\mathbf{k}_L^{b2}] \quad (60)$$

in which the linear axial stiffness matrix is

$$[\mathbf{k}_L^a] = \int_0^l \left\{ \frac{1}{1+\varepsilon_0} [\mathbf{N}']^T \begin{bmatrix} T & 0 \\ 0 & T \end{bmatrix} [\mathbf{N}'] + \frac{EA}{(1+\varepsilon_0)^3} [\mathbf{N}']^T \begin{bmatrix} x_0'^2 & x_0' y_0' \\ x_0' y_0' & y_0'^2 \end{bmatrix} [\mathbf{N}'] \right\} d\bar{s} \quad (61)$$

The linear bending stiffness matrix of the fourth-order derivative is

$$[\mathbf{k}_L^{b1}] = \int_0^l EI [\mathbf{N}''']^T \begin{bmatrix} -y_0'^2 & x_0' y_0' \\ x_0' y_0' & -x_0'^2 \end{bmatrix} [\mathbf{N}'''] d\bar{s} \quad (62)$$

The linear bending stiffness matrix of the third-order derivative is

$$[\mathbf{k}_L^{b2}] = \int_0^l EI \kappa_0 [\mathbf{N}']^T \begin{bmatrix} 2x_0' y_0' & y_0'^2 - x_0'^2 \\ y_0'^2 - x_0'^2 & -2x_0' y_0' \end{bmatrix} [\mathbf{N}'] d\bar{s} \quad (63)$$

Using the standard procedure of the Galerkin finite element method, Eq. (55) leads to the eigenvalue problem, as follows

$$([\mathbf{K}_L] - \omega_i^2 [\mathbf{M}]) \{\bar{\mathbf{D}}\} = \{\mathbf{0}\} \quad (64)$$

where ω_i represents the natural frequency of vibration and $\{\bar{\mathbf{D}}\}$ is the corresponding mode shapes in Cartesian coordinates.

4.2 Nonlinear free vibration solution

The equation of the nonlinear free vibration can be written as

$$[\mathbf{M}]\{\ddot{\mathbf{D}}\} + ([\mathbf{K}_L] + [\mathbf{K}_{NL}])\{\mathbf{D}\} = \{\mathbf{0}\} \quad (65)$$

where $[\mathbf{K}_{NL}]$ is the nonlinear element stiffness matrix, which is the combination of nonlinear axial stiffness matrices and nonlinear bending stiffness matrices.

$$[\mathbf{k}_{NL}] = [\mathbf{k}_{NL}^{a1}] + [\mathbf{k}_{NL}^{a2}] + [\mathbf{k}_{NL}^{b1}] + [\mathbf{k}_{NL}^{b2}] + [\mathbf{k}_{NL}^{b3}] + [\mathbf{k}_{NL}^{b4}] \quad (66)$$

The first-order nonlinear axial stiffness matrix is

$$[\mathbf{k}_{NL}^{a1}] = \int_0^l \frac{EA}{(1+\varepsilon_0)^3} [\mathbf{N}']^T \begin{bmatrix} 3x'_0 u' + y'_0 v' & x'_0 v' + y'_0 u' \\ x'_0 v' + y'_0 u' & 3y'_0 v' + x'_0 u' \end{bmatrix} [\mathbf{N}'] d\bar{s} \quad (67)$$

The second-order nonlinear axial stiffness matrix is

$$[\mathbf{k}_{NL}^{a2}] = \int_0^l \frac{EA}{(1+\varepsilon_0)^3} [\mathbf{N}']^T \begin{bmatrix} \frac{3}{2} u'^2 + \frac{1}{2} v'^2 & u' v' \\ u' v' & \frac{3}{2} v'^2 + \frac{1}{2} u'^2 \end{bmatrix} [\mathbf{N}'] d\bar{s} \quad (68)$$

The first-order nonlinear bending stiffness matrix of the fourth-order derivative is

$$[\mathbf{k}_{NL}^{b1}] = \int_0^l EI [\mathbf{N}''']^T \begin{bmatrix} -2y'_0 v' & y'_0 u' + x'_0 v' \\ y'_0 u' + x'_0 v' & -2x'_0 u' \end{bmatrix} [\mathbf{N}'''] d\bar{s} \quad (69)$$

The second-order nonlinear bending stiffness matrix of the fourth-order derivative is

$$[\mathbf{k}_{NL}^{b2}] = \int_0^l EI [\mathbf{N}''']^T \begin{bmatrix} -v'^2 & u' v' \\ u' v' & -u'^2 \end{bmatrix} [\mathbf{N}'''] d\bar{s} \quad (70)$$

The first-order nonlinear bending stiffness matrix of the third-order derivative is

$$[\mathbf{k}_{NL}^{b3}] = \int_0^l \left\{ 2EI\kappa_0 [\mathbf{N}']^T \begin{bmatrix} y'_0 u' + x'_0 v' & -x'_0 u' + y'_0 v' \\ -x'_0 u' + y'_0 v' & -y'_0 u' - x'_0 v' \end{bmatrix} [\mathbf{N}'''] \right\} d\bar{s} \quad (71)$$

The second-order nonlinear bending stiffness matrix of the third-order derivative is

$$[\mathbf{k}_{NL}^{b4}] = \int_0^l EI [\mathbf{N}']^T \kappa_0 \begin{bmatrix} 2u' v' & -u'^2 + v'^2 \\ -u'^2 + v'^2 & -2u' v' \end{bmatrix} [\mathbf{N}'''] d\bar{s} \quad (72)$$

Using the standard Galerkin finite element method, Eq. (65) leads to the nonlinear eigenvalue problem, as follows

$$\left(([\mathbf{K}_L] + [\mathbf{K}_{NL}]) - \omega_i^2 [\mathbf{M}] \right) \{\bar{\mathbf{D}}\} = \{\mathbf{0}\} \quad (73)$$

where ω_i represents the natural frequency of vibration and $\{\bar{\mathbf{D}}\}$ is the corresponding mode shapes in Cartesian coordinates.

The expression of the nonlinear equation of motion in Eq. (73) is time dependent; therefore, to reduce it to a time-independent nonlinear eigenvalue problem, the certain properties of the time function are substituted to the point of the maximum amplitude or the point of reversal of the motion.

The dynamic displacement is assumed by substitution of the characteristic of the time function as an instant with harmonic function to obtain the eigenvalue problem (Sarma and Varadan 1982)

$$\{\ddot{\mathbf{D}}\}_{max} = -\omega_i^2 \{\mathbf{D}\}_{max} \quad (74)$$

where ω_i is the natural frequencies of the catenary riser and $\{\mathbf{D}\}_{max}$ is the dynamic displacement at the nodal point of maximum amplitude.

The equation of motion for time-independent, large-amplitude free vibration is obtained by substitution of Eq. (74) into Eq. (65), as follows

$$\left(([\mathbf{K}_L] + [\mathbf{K}_{NL}]) - \omega_i^2 [\mathbf{M}] \right) \{\mathbf{D}\}_{max} = \{\mathbf{0}\} \quad (75)$$

The relationship between the dynamic displacements of the catenary riser at the point of maximum amplitude as expressed in Eq. (75) and the vibration mode shape can be expressed by

$$\{\mathbf{D}\}_{max} = a\{\mathbf{V}\} \quad (76)$$

where a is the maximum amplitude of vibration and $\{\mathbf{V}\}$ is the normalized corresponding mode shapes.

5. Numerical results

The free vibration of the catenary riser is validated with the numerical results proposed by Chuchepsakul and Huang (1989) to verify the effectiveness of the proposed model formulation. The water depth of the catenary riser is 400 m and the offset distance varies from 20 m to 120 m. The outside diameter is 0.55 m, the inside diameter is 0.50 m, and the densities of the steel, seawater, and internal fluid are 7850 kg/m³, 1025 kg/m³, and 1410 kg/m³, respectively. The values of the top tension and elastic modulus are 1700 kN and 2.10 x 10⁸ kN/m², respectively, and the added mass coefficient is 1.0.

The convergence evaluation of the riser problem in this validation with 20 m offset distance are performed using 10, 15, 20, 30, 40, 60 and 80 elements discretization. The finite element analysis with 40 equal elements discretization provided sufficiently accurate results as presented in Table 1. Therefore, 40 equal elements were used throughout to conduct finite element analysis.

The natural frequencies of the first three mode shapes of the catenary riser with varying offset distances from 20 m to 120 m are illustrated in Table 2 and were found to be in good agreement with the reference research work. The first three mode shapes of the catenary riser with 20 m offset distance are shown in Fig. 3.

Table 1 Convergence evaluation

Mode (rad/sec)	Mode 1		Mode 2		Mode 3	
Elements discretization	Natural frequencies	Difference	Natural frequencies	Difference	Natural frequencies	Difference
10	0.453823	-	0.730382	-	0.967309	-
15	0.454013	0.042%	0.730578	0.027%	0.967604	0.031%
20	0.454037	0.005%	0.730607	0.004%	0.967625	0.002%
30	0.454045	0.002%	0.730618	0.002%	0.967629	0.000%
40	0.454046	0.000%	0.730619	0.000%	0.967630	0.000%
60	0.454046	0.000%	0.730620	0.000%	0.967630	0.000%
80	0.454046	0.000%	0.730620	0.000%	0.967630	0.000%

Table 2 Natural frequencies of the catenary riser for various offset distances

Mode (rad/sec)	Mode 1		Mode 2		Mode 3	
Offset (m)	This study	FEM ^(a)	This study	FEM ^(a)	This study	FEM ^(a)
20	0.454	0.456	0.731	0.728	0.968	0.960
30	0.465	0.467	0.778	0.777	1.141	1.139
40	0.465	0.469	0.786	0.786	1.167	1.166
60	0.460	0.466	0.781	0.784	1.160	1.162
80	0.451	0.460	0.770	0.775	1.143	1.147
120	0.425	0.445	0.734	0.750	1.091	1.106

Note: FEM^(a) = Chucheepsakul and Huang (1989)

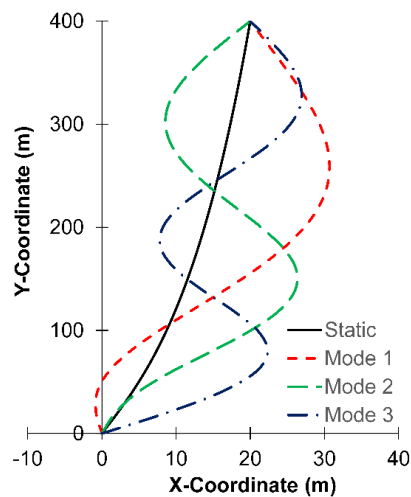


Fig. 3 Mode shapes of the catenary riser

Table 3 Natural frequencies of the catenary riser supported at the same elevation

Mode (rad/sec)	$T_H = 500$ kN	$T_H = 100$ kN	$T_H = 50$ kN	$T_H = 30$ kN
1	1.1764	0.5098	0.3373	0.2403
2	1.2194	0.7624	0.5505	0.4388
3	1.8316	1.0644	0.7710	0.6244
4	2.3585	1.3239	0.9749	0.8012

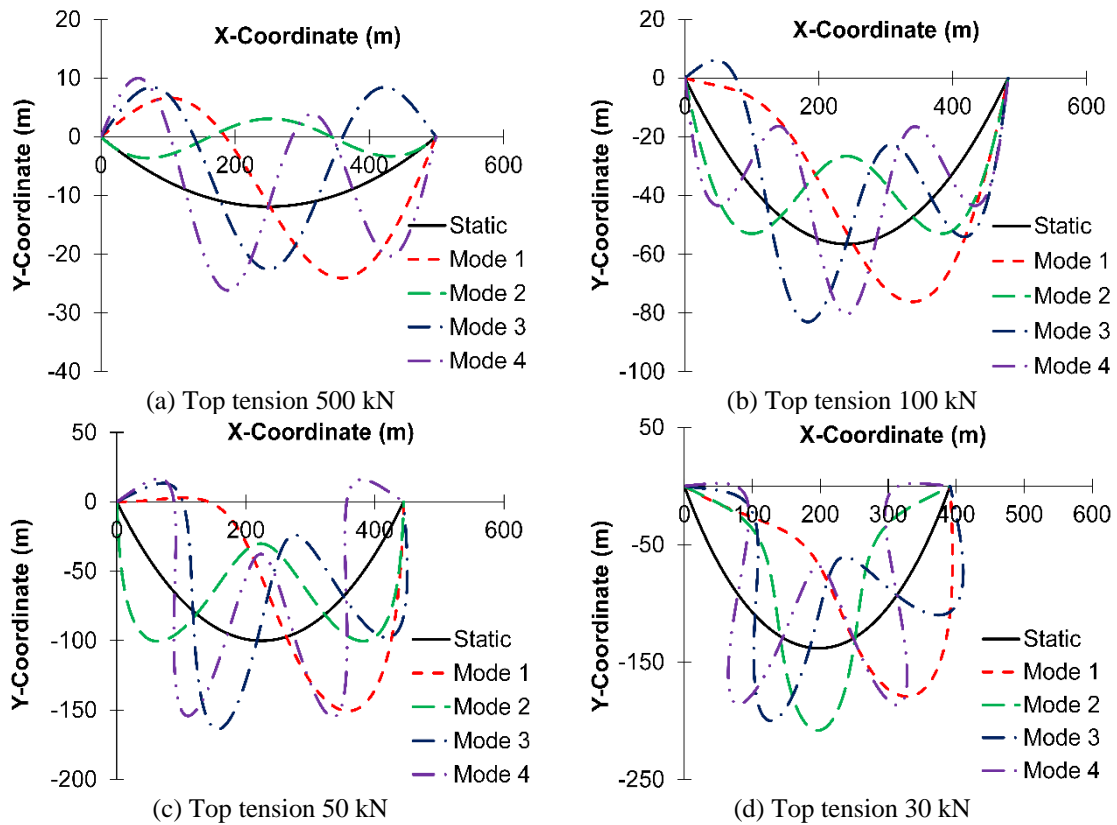


Fig. 4 Mode shapes of the catenary riser supported at the same elevation

The numerical result for the free vibration analysis of the large-sag extensible catenary riser is presented in this section. The input parameters are the external diameter, internal diameter, and the unstrained arc length, which are 0.1524 m, 0.1397 m, and 500 m, respectively. The densities of the riser, seawater, and internal fluid are 7850 kg/m³, 1025 kg/m³, and 998 kg/m³, respectively. The elastic modulus is 2.07 x 10⁸ kN/m², the current velocity is 1.0 m/s, and the added mass coefficient is 1.0. The applied top horizontal tension varied, with values equal to 500, 100, 50, and 30 kN.

Table 3 presents the natural frequencies of the first four mode shapes of the catenary riser supported at the same elevation for the top horizontal tensions 500, 100, 50, and 30 kN. The numerical results show that the natural frequency decreases as the top horizontal tension decreases.

Table 4 Natural frequencies of the catenary riser supported at different elevations

Mode (rad/sec)	$T_H = 500$ kN	$T_H = 100$ kN	$T_H = 50$ kN	$T_H = 30$ kN
1	1.1833	0.5159	0.3429	0.2462
2	1.1977	0.7710	0.5574	0.4435
3	1.8416	1.0757	0.7789	0.6299
4	2.3828	1.3377	0.9843	0.8076

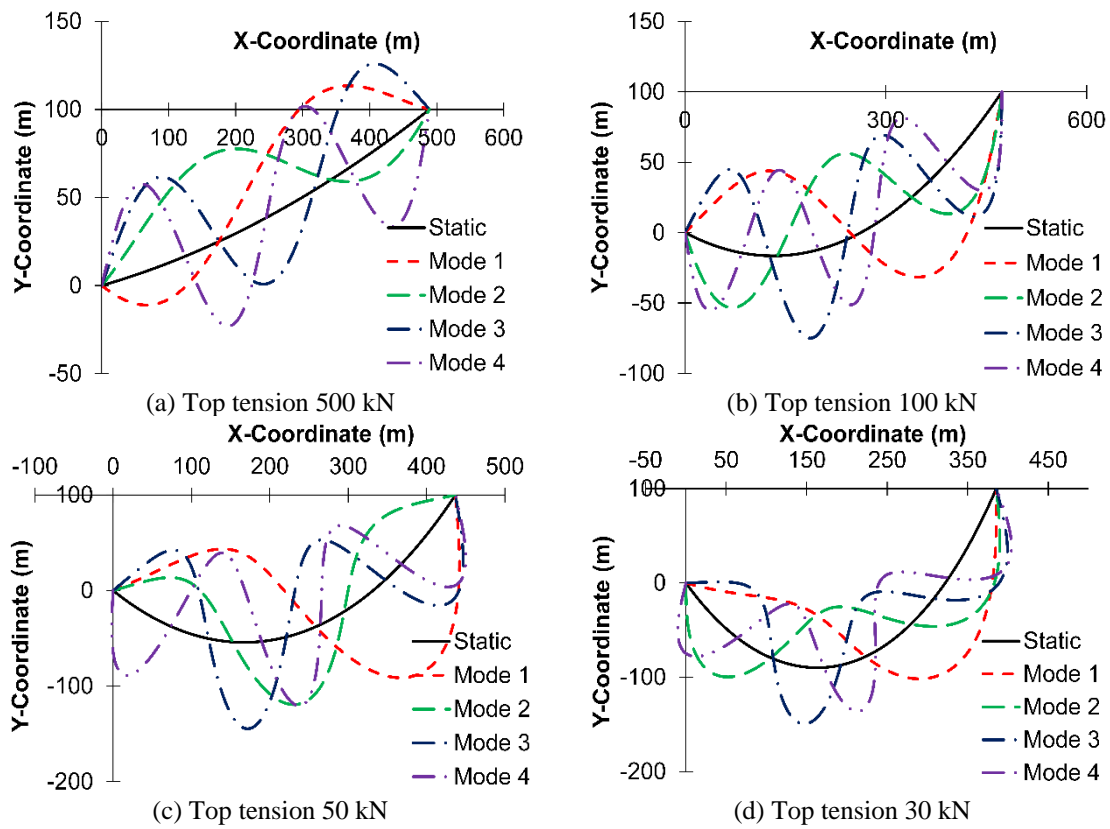


Fig. 5 Mode shapes of the catenary riser supported at different elevations

The first four mode shapes for the catenary riser with both supports at the same elevation, with applied top horizontal tension of 500 kN, 100 kN, 50 kN, and 30 kN, are illustrated in Figs. 4(a)-4(d), respectively.

The results for natural frequencies of the catenary riser with the support elevation of 100 m are as presented in Table 4. It was found that the natural frequency decreases as top horizontal tension decreases. The first four mode shapes for the catenary riser with 100 m support elevation and applied top horizontal tension of 500 kN, 100 kN, 50 kN, and 30 kN are illustrated in Figs. 5(a)-5(d), respectively.

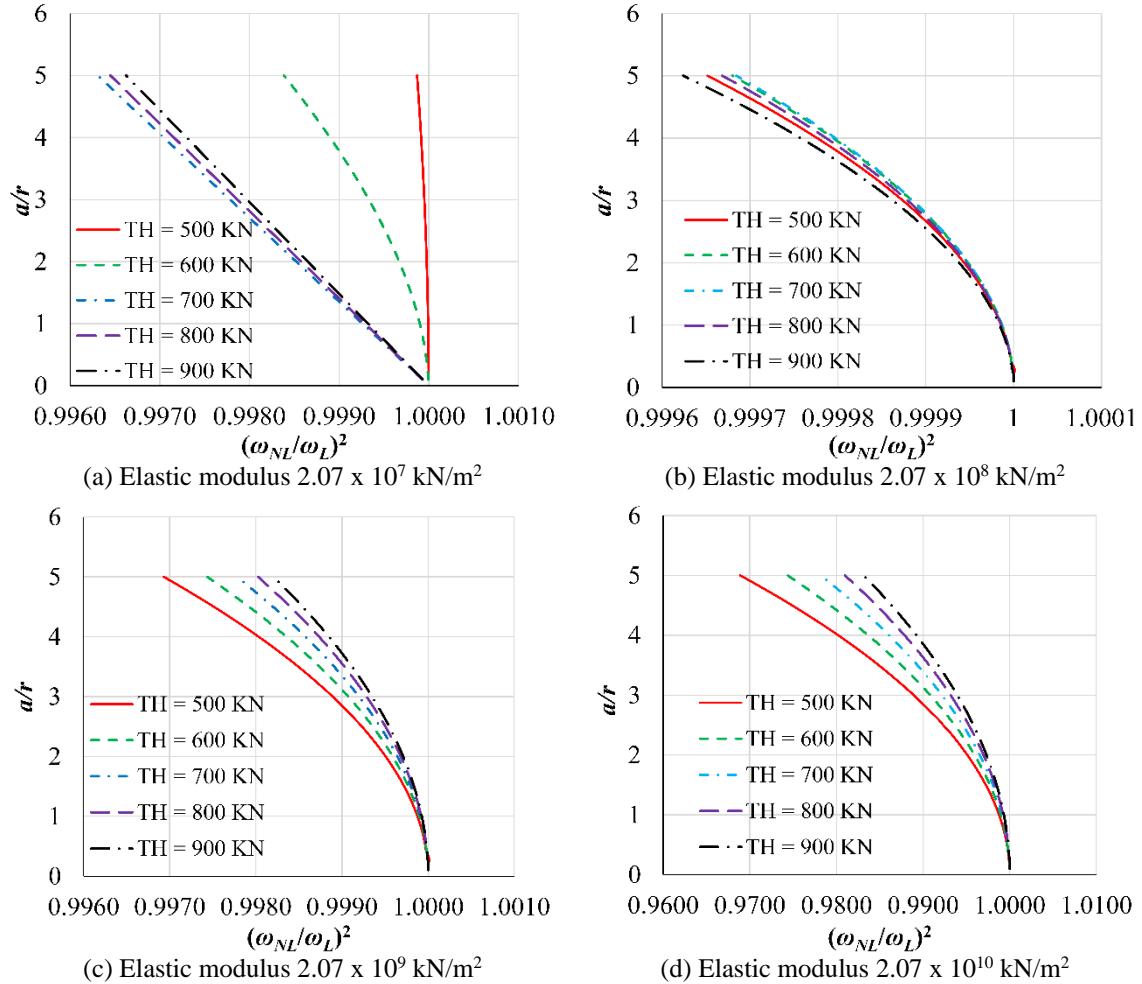


Fig. 6 Effect of the top horizontal tension on the relationship between nonlinear frequency ratios $(\omega_{NL}/\omega_L)^2$ and amplitude of vibration (a/r) for catenary riser supports at the same elevation and elastic modulus values of 2.07×10^7 kN/m² to 2.07×10^{10} kN/m²

In this section, the effect of nonlinear axial and bending stiffness matrices based on the proposed equations of motion for the large-sag extensible catenary riser is investigated. The input parameters are the external diameter, internal diameter, and the unstrained arc length, which are 0.1524 m, 0.1397 m, and 2000 m, respectively. The densities of the riser, seawater, and internal fluid are 7850 kg/m³, 1025 kg/m³, and 998 kg/m³, respectively. The elastic modulus varies from 2.07×10^7 kN/m² to 2.07×10^{10} kN/m², the current velocity is 1.0 m/s, and the added mass coefficient is 1.0. The applied top horizontal tension varied, with values equal to 500 kN to 900 kN. The support elevation was considered as the same elevation and 1000 m support elevation. The results of nonlinear free vibration analysis between the frequency ratio $(\omega_{NL}/\omega_L)^2$ and amplitude of vibration (a/r) are plotted in Fig. 6 for the support at the same elevation and Fig. 7 for the support elevation of 1000 m, where ω_{NL} is the nonlinear frequency and ω_L is the linear frequency, obtained from the nonlinear

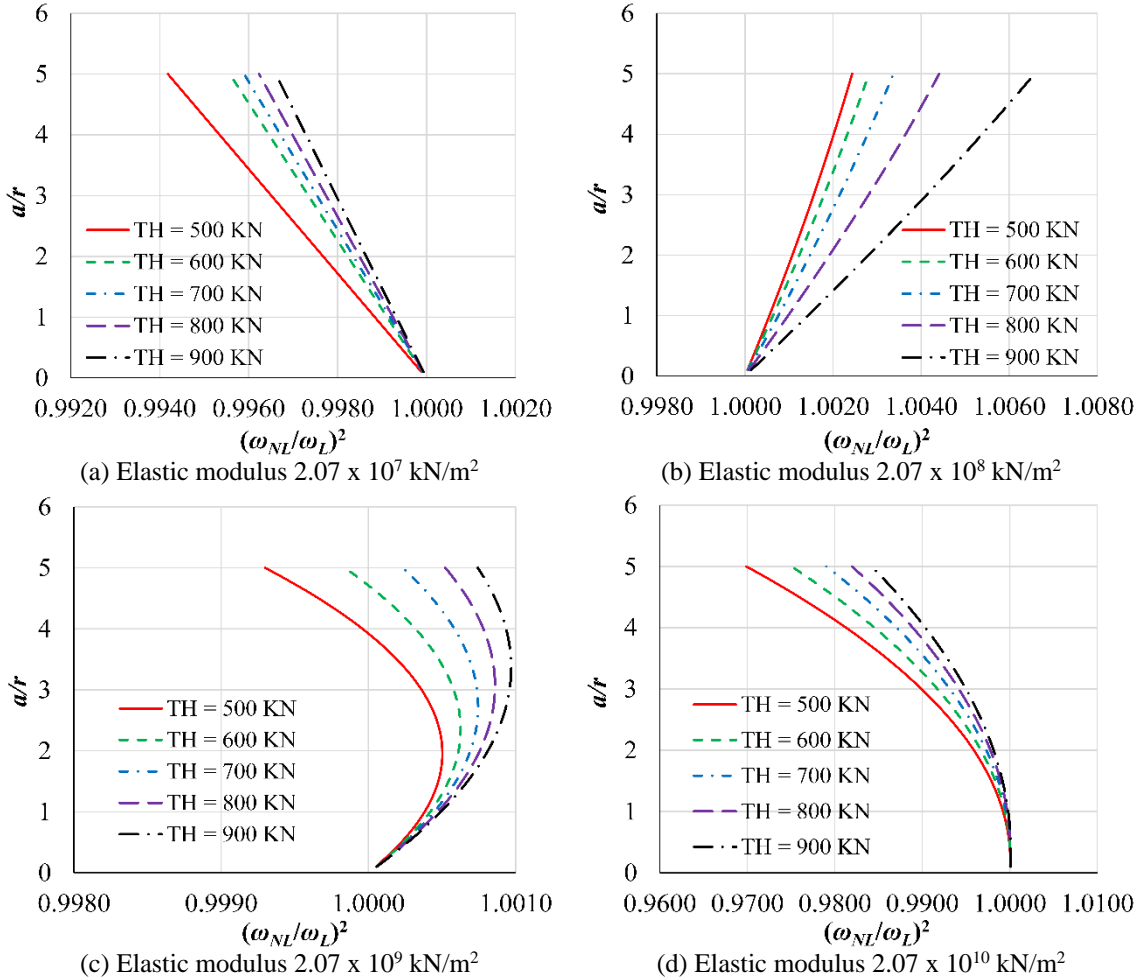


Fig. 7 Effect of the top horizontal tension on the relationship between nonlinear frequency ratios $(\omega_{NL}/\omega_L)^2$ and amplitude of vibration (a/r) for catenary riser supports with elevation 1000 m and elastic modulus values of 2.07×10^7 kN/m² to 2.07×10^{10} kN/m²

free vibration analysis and linear free vibration analysis, respectively, and r is the radius of gyration of the catenary riser.

Figs. 6 and 7 exhibit the behavior of nonlinear free vibration depends on the parameters of support elevation, top horizontal tension value and elastic modulus values as presented in section 5.1, 5.2 and 5.3, respectively.

5.1 Effect of support elevation

The results for nonlinear free vibration of the large-sag extensible catenary riser suspended at the same elevation of support exhibit the behavior of nonlinear free vibration as a softening type for all values of the elastic modulus, as illustrated in Figs. 6(a) to 6(d). For the catenary riser with support

elevation of 1000 m, the nonlinear free vibration behavior exhibits a softening type for the elastic modulus of 2.07×10^7 kN/m² and 2.07×10^{10} kN/m², as shown in Figs. 7(a) and 7(d), while the elastic modulus value of 2.07×10^8 kN/m² exhibits the hardening type of nonlinear free vibration behavior, as shown in Fig. 7(b). The elastic modulus value of 2.07×10^9 kN/m² exhibits the nonlinear frequency ratio moving from hardening to softening type, as shown in Fig. 7(c).

5.2 Effect of top horizontal tension

The effect of top horizontal tension on the nonlinear free vibration behavior of the extensible catenary riser with the support at the same elevation is illustrated in Fig. 6. The results show the degree of softening increases as the top horizontal tension increases, as shown in Figs. 6(a) and 6(b) for the elastic modulus values of 2.07×10^7 kN/m² and 2.07×10^8 kN/m², respectively, while the degree of softening increases as the top horizontal tension decreases, as shown in Figs. 6(c) and 6(d) for the elastic modulus of 2.07×10^9 kN/m² and 2.07×10^{10} kN/m², respectively.

For the catenary riser with the support elevation set to 1000 m, the nonlinear free vibration behavior exhibits a softening type for the elastic modulus of 2.07×10^7 kN/m² and 2.07×10^{10} kN/m². The results presented show that the degree of softening increases as the top horizontal tension values decrease, as shown in Figs. 7(a) and 7(d), respectively. The elastic modulus values of 2.07×10^8 kN/m² and 2.07×10^9 kN/m² in Figs. 7(b) and 7(c), respectively, exhibit the hardening type of nonlinear free vibration behavior and the degree of hardening increases as the top horizontal tension value increases.

5.3 Effect of elastic modulus

The nonlinear free vibration behavior of the extensible catenary riser with the support at the same elevation exhibits a softening type for all values of elastic modulus as illustrated in Fig. 6(a) to 6(d). The degree of softening increases as the elastic modulus value increases. The nonlinear free vibration behavior of the catenary riser with support elevation of 1000 m exhibits a softening type for the elastic modulus values of 2.07×10^7 kN/m² and 2.07×10^{10} kN/m², and the plotted values show a hardening type of nonlinear free vibration behavior for the elastic modulus values of 2.07×10^8 kN/m² and 2.07×10^9 kN/m².

6. Conclusions

The nonlinear model formulation based on the variational approach for free vibration of a large-sag extensible catenary riser using the arc length coordinate adopted from the Lagrangian description as the independent variable are presented in this paper. The total virtual work due to axial deformation and bending strain energy and virtual work due to effective weight and inertia forces were addressed. The equations of motion were derived from the difference between the Euler's equations in the static state and the displaced state. The linear and nonlinear stiffness matrices of the catenary riser are obtained. Finally, the eigenvalue problem of linear free vibration analysis was solved by the inverse iteration method to obtain the natural frequencies and corresponding mode shapes, while the direct iteration method was used for nonlinear free vibration analysis.

The numerical results for free vibration of the large-sag catenary riser was validated and found to be in good agreement with the reference research work. The free vibration of the large-sag

extensible catenary riser with the support at the same and different elevations was performed while varying the top horizontal tension. The numerical results show the natural frequencies decrease as the top horizontal tension decreases. The nonlinear behavior based on the proposed formulation for the large-sag extensible catenary riser is investigated with various parameters and discussed herein.

References

- Alfosail, F.K., Nayfeh, A.H. and Younis, M.I. (2017), "Natural frequencies and mode shapes of statically deformed inclined risers," *Int. J. Nonlin. Mech.*, **94**, 12-19. <https://doi.org/10.1016/j.ijnonlinmec.2016.09.007>.
- Athisakul, C., Klaycham, K. and Chucheepsakul, S. (2014), "Critical top tension for static equilibrium configuration of a steel catenary riser", *China Ocean Eng.*, **28**(6), 829-842. <https://doi.org/10.1007/s13344-014-0064-x>.
- Athisakul, C., Monprapussorn, T. and Chucheepsakul, S. (2011), "A variational formulation for three-dimensional analysis of extensible marine riser transporting fluid", *Ocean Eng.*, **38**, 609-620. <https://doi.org/10.1016/j.oceaneng.2010.12.012>.
- Chatjigeorgiou, I.K. (2008), "A finite differences formulation for the linear and nonlinear dynamics of 2D catenary risers", *Ocean Eng.*, **35**, 616-636. <https://doi.org/10.1016/j.oceaneng.2008.01.006>.
- Chucheepsakul, S. and Huang, T. (1989), "Natural frequencies of a marine riser in three-dimensions", *Proceedings of the 7th Int. Offshore Mech. Arct. Eng. Symposium*.
- Chucheepsakul, S., Monprapussorn, T. and Huang, T. (2003), "Large strain formulations of extensible flexible marine pipes transporting fluid", *J. Fluid Struct.*, **17**, 185-224. [http://dx.doi.org/10.1016/S0889-9746\(02\)00116-0](http://dx.doi.org/10.1016/S0889-9746(02)00116-0).
- Cook, R.D., Malkus, D.S. and Plesha, M.E. (2002), *Concept and Applications of Finite Element Analysis*, 4th Ed., Wiley & Sons, New York.
- Kaewunruen, S., Chiravatchradej, J. and Chucheepsakul, S. (2005), "Nonlinear free vibrations of marine risers/pipes transporting fluid", *Ocean Eng.*, **32**, 417-440. <https://doi.org/10.1016/j.oceaneng.2004.07.007>.
- Kim, H.T. and O'Reilly, O.M. (2019), "Instability of catenary-type flexible risers conveying fluid in subsea environments", *Ocean Eng.*, **173**, 98-115. <https://doi.org/10.1016/j.oceaneng.2018.12.042>.
- Klaycham, K. (2016), "Nonlinear vibrations of extensible marine risers", Doctor of Philosophy Dissertation, Civil Engineering Program, King's Mongkut University of Technology Thonburi.
- Klaycham, K., Athisakul, C. and Chucheepsakul, S. (2014), "Nonlinear free vibration of a steel catenary riser", *Proceedings of the 24th Int. Ocean and Polar Eng. Conf.*, Busan, Korea.
- Klaycham, K., Athisakul, C. and Chucheepsakul, S. (2016), "Nonlinear vibration of marine riser with large displacement", *J. Mar. Sci. Tech.*, 1-15. <https://doi.org/10.1007/s00773-016-0416-8>.
- Klaycham, K., Nguantud, K., Athisakul, C. and Chucheepsakul, S. (2020), "Free vibration analysis of large sag catenary with application to catenary jumper", *Ocean Syst. Eng.*, **10**(1), 67-86. <https://doi.org/10.12989/ose.2020.10.1.067>.
- Moe, G., and Arntsen, O. (2001), "An analytic model for static analysis of catenary risers", *Proceedings of the 11th Int. Offshore and Polar Eng. Conf.*, Stavanger, Norway, 248-253.
- Monprapussorn, T., Athisakul, C. and Chucheepsakul, S. (2007), "Nonlinear vibrations of an extensible flexible marine riser carrying a pulsatile flow", *J. Appl. Mech.*, **74**(4), 754-769. <https://doi.org/10.1115/1.2711226>.
- Pesce, C.P., Aranha, J.A.P., Martins, C.A., Ricardo, O.G.S. and Silva, S. (1998), "Dynamic curvature in catenary risers at touchdown point: An experimental study and boundary-layer solution", *Int. J. Offshore Polar Eng.*, **8**(4), 303-310.
- Punjarat, O. and Chucheepsakul, S. (2019a), "Post-buckling model for uniform self-weight beam with an application to catenary riser", *Int. J. Struct. Stab. Dyn.*, **19**(4), 1-21. <http://dx.doi.org/10.1142/S0219455419500470>.

- Punjarat, O. and Chucheeepsakul, S. (2019b), "Free vibration of a very-large-sag extensible catenary riser", *Proceedings of the 2019 World Congress on Adv. Struct. Eng. Mech.*, Korea.
- Sarma, B.S. and Varadan, T.K. (1982), "Certain discussions in the finite element formulation of nonlinear vibration analysis", *Comput. Struct.*, **15**(6), 61-70. [https://doi.org/10.1016/S0045-7949\(82\)80004-7](https://doi.org/10.1016/S0045-7949(82)80004-7).
- Srinil, N., Wiercigroch, M. and O'Brien, P. (2009a), "Reduced-order modelling of vortex-induced vibration of catenary riser", *Ocean Eng.*, **36**, 1404-1414. <https://doi.org/10.1016/j.oceaneng.2009.08.010>.
- Srinil, N., Wiercigroch, M., O'Brien, P. and Younger, R. (2009b), "Vortex-induced vibration of catenary riser: Reduced-order modeling and lock-in analysis using wake oscillator", *Proceedings of the ASME 28th Int. Conference on Ocean, Offshore and Arctic Eng. OMAE*, Honolulu, Hawaii.
- Zou, J. (2012), "Semisubmersible platforms with Steel Catenary Risers for Western Australia and Gulf of Mexico", *Ocean Sys. Eng.*, **2**(2), 99-113. <http://dx.doi.org/10.12989/ose.2012.2.2.099>.

MK